The pK_a of His-24 in the folding transition state of apomyoglobin

Marc Jamin*, Bernhard Geierstanger†, and Robert L. Baldwin§

Department of Biochemistry, Beckman Center, Room B400, Stanford University Medical Center, Stanford, CA 94305-5307

Contributed by Robert L. Baldwin, March 30, 2001

In native apomyoglobin, His-24 cannot be protonated, although at pH 4 the native protein forms a molten globule folding intermediate in which the histidine residues are readily protonated. The inability to protonate His-24 in the native protein dramatically affects the unfolding/refolding kinetics, as demonstrated by simulations for a simple model. Kinetic data for wild type and for a mutant lacking His-24 are analyzed. The pK_a values of histidine residues in native apomyoglobin are known from earlier studies, and the average histidine pK_a in the molten globule is determined from the pH dependence of the equilibrium between the native and molten globule forms. Analysis of the pH-dependent unfolding/refolding kinetics reveals that the average pK_a of the histidine residues, including His-24, is closely similar in the folding transition state to the value found in the molten globule intermediate. Consequently, protonation of His-24 is not a barrier to refolding of the molten globule to the native protein. Instead, the normal pK_a of His-24 in the transition state, coupled with its inaccessibility in the native state, promotes fast unfolding at low pH. The analysis of the wild-type results is confirmed and extended by using the wild-type parameters to fit the unfolding kinetics of a mutant lacking His-24.

His-24 plays a remarkable role in the structure and pH titration behavior of apomyoglobin (apoMb). His-24, which is in the B helix, is completely buried, and its neutral imidazole ring is hydrogen bonded to that of His-119 in the G helix (1–3), thus providing a strong link (4) between the B and G helices. Although His-119 can be protonated at low pH, His-24 remains neutral and cannot be protonated in the native form (N) of apoMb (2). The charged guanidinium group of Arg-118 sits directly above the imidazole ring of His-24 in N (5). Consequently, protonation of His-24 occurs only when N forms a stable molten globule intermediate (I) at pH 4. Only a subdomain of N containing the A, G, and H helices of apoMb is stably folded in I (6).

His-48, His-64, His-113, and His-119 have low pK_a values in N (2, 7), but only His-24 is entirely resistant to being protonated in N; and protonation of His-24 at pH 4 forces the conversion of N to I. All histidine residues are protonated in the molten globule at and below pH 5, where I is formed (2); thus, the pK_a values of all histidines in the molten globule are close to normal.

Because His-24 cannot be protonated in N, the question arises of whether His-24 can be protonated in the folding transition state ($I^{\ddagger}$) of the N to I reaction. Barrick *et al*. (4) pointed out that, if His-24 is inaccessible in the folding transition state, this will present a serious kinetic barrier to the refolding of I to N at pH values where I is protonated. To answer this question, we first determine the average pK_a value of the histidine residues in the molten globule, from the pH-dependent equilibrium between N and I, using data from ref. 8, combined with the pK_a values of histidine residues in the native state, determined earlier (2, 7). The N $\rightleftharpoons$ I equilibrium depends on pH through ΔQ, the difference between the number of protons bound to N vs. I, and the pH dependence of its standard free energy is given by $-2.303\int \Delta Q\,dpH$. This integral is calculable from the pK_as of the histidines in N and I (9) when unfolding occurs in the pH range in which only histidines are titrating. We use the extensive data of Barrick and Baldwin (8) on the pH dependence of the equilibrium [N]/[I] ratio.

After determining the average pK_a value of histidines in the molten globule intermediate, the average pK_a value of histidines in the folding transition state may be calculated from the plot of log k_{obs} vs. pH (9, 10), because the pK_a values in N and I are known. Simulations reveal that, if any histidine has a pK_a in the folding transition state that differs markedly from the average value, this fact will be apparent in the pH dependence of the unfolding/refolding kinetics.

The double mutant H24V/H119F (4) provides an important control for this analysis of the unfolding/refolding kinetics of wild type (WT). The double mutant is stably folded: the double replacement of His-24 and His-119 with Val and Phe is found commonly in the globin family, and the nonpolar Val-Phe link between the B and G helices makes the double mutant more stable to urea unfolding at neutral pH than WT (4). The single mutants H24V and H119F are both considerably less stable than WT (4). The main cause for the WT native state's becoming unstable at low pH is the protonation of His-24 in I, and, because the double mutant lacks His-24, its N $\rightleftharpoons$ I unfolding transition is shifted down near pH 3, where the Asp and Glu residues undergo protonation (2, 4). The unfolding transition of the less stable mutant H36Q, which also is studied here, is shifted in the opposite direction to a higher pH range because protonated His-36 stabilizes WT through side chain interactions (4).

Experimental Procedures

Protein Expression and Purification. A synthetic gene for sperm whale myoglobin was expressed and purified as described (2, 11). The heme was removed by acid-acetone precipitation (12). Protein concentration was determined by absorbance in 6 M GdmCl as described (13) using $\varepsilon_{280\ nm} = 15{,}200\ M^{-1}\cdot cm^{-1}$ and $\varepsilon_{288\ nm} = 10{,}800\ M^{-1}\cdot cm^{-1}$.

Fluorescence Stopped-Flow Experiments. Data were collected on an Applied Photophysics (Surrey, U.K.) model DX17 MV instrument, using a 2-mm pathlength cell. Excitation was at 288 nm, and measurements of emission were made by using an optical cutoff filter. Kinetic traces from the stopped-flow experiments were fitted to single, double, and triple exponential time courses with the software provided by Applied Photophysics.

Modeling the pH Dependence of the Rate Constants. All simulations were performed with SIGMAPLOT (Jandel, San Rafael, CA). The

Abbreviations: N, native form; I, folding intermediate; $I^{\ddagger}$, folding transition state; U, acid-unfolded form; WT, wild type; ΔQ, difference in number of protons bound to N and I; pH_m, pH midpoint of unfolding transition; ΔG_{NI}, difference in standard Gibbs free energy between N and I; apoMb, apomyoglobin.

*Present address: Laboratoire de Biophysique Moleculaire et Cellulaire, DBMS/BMC CEA-Grenoble, 17 rue des Martyrs, Grenoble 38054, France.

†Present address: Genomics Institute of the Novartis Research Foundation, 3115 Merryfield Row, Suite 200, San Diego, CA 92121-1125.

§E-mail: bbaldwin@cmgm.stanford.edu.

The publication costs of this article were defrayed in part by page charge payment. This article must therefore be hereby marked "*advertisement*" in accordance with 18 U.S.C. §1734 solely to indicate this fact.

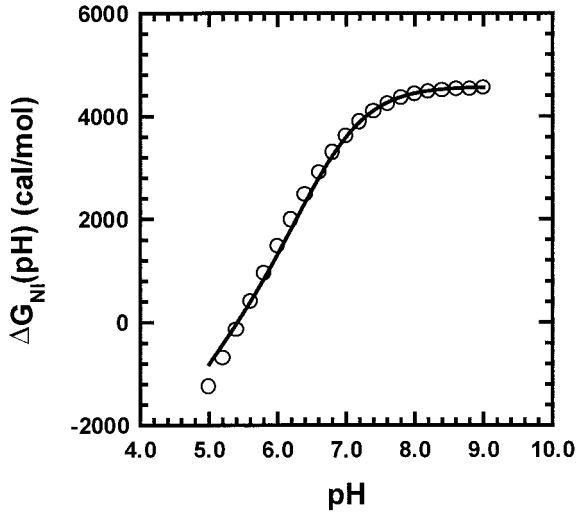

Fig. 1. Determination at 0°C of the average pK_a of histidines in the molten globule (see text for details). Values of ΔG_{NI}, the change in Gibbs energy for unfolding from N to I, are taken from ref. 8. The fitted curve is given by -2.303 $\int\Delta Q$ dpH, where ΔQ is the difference in number of protons bound to N vs. I; ΔQ is computed from the pK_a values in N measured by chemical shift titration (2,7) and from the average pK_a in I, treated as the sole unknown.

rate constants for folding (k_f) and unfolding (k_u) are expressed as functions of pH by assuming that the proton binding sites are independent, using the following equations.

$$k_f = k_f^{ref}\frac{\prod[1 + 10^{\wedge}(pK_{ai}^{\ddagger} - pH)]}{[1 + 10^{\wedge}(pK_{ai}^{Ib} - pH)]} \quad [1a]$$

$$k_u = k_u^{ref}\frac{\prod[1 + 10^{\wedge}(pK_{ai}^{\ddagger} - pH)]}{\prod[1 + 10^{\wedge}(pK_{ai}^{N} - pH)]} \quad [1b]$$

$$K = \frac{k_f}{k_u}, \quad [2]$$

where k_f^{ref} and k_u^{ref} are the reference rate constants for the Ib $\rightarrow$ N and N $\rightarrow$ Ib reactions, respectively, at pH 9; K is the folding equilibrium constant; and the pK_{ai} values refer to residue i in the N, Ib, and I‡ forms.

Results

Average pK_a of Histidines in the Molten Globule. Fig. 1 shows ΔG_{NI}(pH), the difference in standard Gibbs free energy between N and I, calculated from data given by Barrick and Baldwin (8), who used circular dichroism to measure the pH-induced and urea-induced unfolding transitions of apoMb at 0°C from pH 1 to 8 and from 0 to 8 M urea. They fitted the results to a simplified three-state model (N $\rightleftharpoons$ I $\rightleftharpoons$ U) using a minimal number of parameters. The urea- and pH-induced unfolding results are fitted closely by the three-state model, and the fitting parameters can be used to give reasonably accurate values of ΔG_{NI}(pH) as a function of pH.

In Fig. 1, ΔG_{NI}(pH) is plotted against pH, and the fitted line is -2.303 $\int\Delta Q$dpH, where ΔQ is computed from the known individual pK_a values of the histidines in N and from the average pK_a of the histidines in I, treated as the sole unknown. The pK_a values in N are corrected to 0°C [the temperature used by Barrick and Baldwin (8)] from the 35°C values of Geierstanger *et al.* (2) by using the heat of protonation of free histidine, -6.9 kcal/mol (14), in the van't Hoff relation. The average pK_a in I is found by least-squares fitting to be 6.8 (0°C). His-36 is omitted from the calculation of $\int\Delta Q$dpH in Fig. 1 because its protonated form stabilizes N, contrary to the assumptions of the simple three-state model, and as a result the contribution of His-36 to the experimental N $\rightleftharpoons$ I data is smoothed out in fitting the data to the model of ref. 8. The native pK_a determinations of histidine residues were made in 10 mM acetate buffer (2) whereas data for the N $\rightleftharpoons$ I unfolding transition (8) were obtained in 2 mM citrate buffer. We show below that, although there is a significant difference in ΔG_{NI} in these two buffers, the same pK_a values apply in both buffers.

Unfolding and Refolding Kinetics vs. pH. Although the nature of the rate equation for protein folding is still under discussion (15), there is general agreement that the transition state approximation provides the basis for the rate equation: it specifies that the folding transition state I‡ is in equilibrium with the denatured protein in refolding and with the native protein in unfolding. There are two forms of the apoMb molten globule, Ia and Ib, which coexist in a pH-dependent equilibrium, and the kinetics of the overall folding reaction indicate that the pathway is N $\rightleftharpoons$ Ib $\rightleftharpoons$ Ia $\rightleftharpoons$ U, in which N is formed directly from Ib, not Ia (16); U is the acid-unfolded form. The designation "I" is used here as a collective term for (Ia,Ib) when both forms are present and no further specification is needed.

In refolding to N, I‡ equilibrates with Ib, and the pH dependence of the folding rate k_f is attributed to this equilibrium:

$$Ib \rightleftharpoons I^{\ddagger} \rightarrow N \quad [3a]$$

$$k_f = K_{I\ddagger}k_{\ddagger N}. \quad [3b]$$

$K_{I\ddagger}$ is the equilibrium constant for equilibration between Ib and I‡, and $k_{\ddagger N}$ is the rate constant with which I‡ breaks down to give N. Likewise, in unfolding to Ib, N equilibrates with I‡, and the unfolding rate k_u is written

$$N \rightleftharpoons I^{\ddagger} \rightarrow Ib \quad [4a]$$

$$k_u = K_{N\ddagger}k_{\ddagger I} \quad [4b]$$

In fitting the experimental curve of log k_{obs} vs. pH, $K_{I\ddagger}$ is pH dependent in refolding experiments, and $K_{N\ddagger}$ is pH dependent in unfolding experiments because these equilibrium constants depend on the pK_a values of residues that titrate in this pH range. For a two-state reaction, the observed rate constant k_{obs} is the sum of the unfolding and refolding rate constants.

$$k_{obs} = k_u + k_f \quad [5]$$

Fig. 2 shows k_{obs} plotted against pH at 4.5°C, in citrate buffer, for WT (Fig. 2*A*) and for the double mutant H24V/H119F (Fig. 2*B*). The average pK_a of histidine residues in the folding transition state, determined from the WT curve, is 6.7, almost the same as in the molten globule (6.8, Table 1). Simulations presented below show that, if His-24 had an abnormally low pK_a in I‡ as it does in N, this would be readily observable from the shape of the curve of log k_{obs} vs. pH. Exactly the same parameters are used to fit the WT curve and the H24V/H119F curve (Fig. 2*B*), whereas the pK_a values of His-24 and His-119 are omitted in the latter. The pK_a values used to fit these curves (Table 1) are discussed below.

Results in Acetate Buffer. Because citrate buffer causes the Ia $\rightleftharpoons$ Ib equilibrium to be more strongly dependent on pH than acetate buffer (ref. 16 and unpublished results), and because we thought this behavior might affect the pH dependence of the unfolding/refolding kinetics, we also determined the unfolding/refolding kinetics in 10 mM acetate buffer. Fig. 3 shows the results for WT (Fig. 3*A*) and two mutants (H24V/H119F), whose unfolding curve is shifted to lower pH (Fig. 3*B*), and H36Q (Fig. 3*C*), whose unfolding curve is shifted to higher pH. These curves are

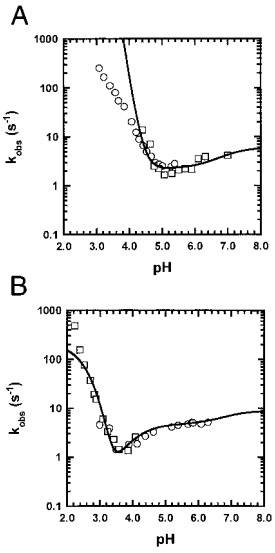

Fig. 2. The plot of log k_{obs} vs. pH for pH-induced unfolding/refolding in a citrate buffer (2 mM citrate/30 mM NaCl) at 4.5°C for WT (*A*) and the double mutant H24V/H119F (*B*). Both mutant and WT curves are fitted by using the same pK_a values (Table 1), with reference values $k_u = 0.001$ and $k_f = 6$ (*A*) or with $k_u = 2 \times 10^{-5}$ and $k_f = 9$ (*B*). The rate constants are given in units of s^{-1} and the reference values refer to pH 9.

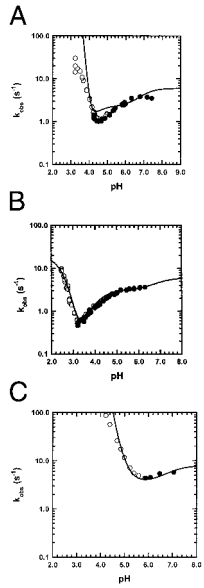

Fig. 3. The plot of log k_{obs} vs. pH in 10 mM acetate buffer at 4.5°C for WT (*A*), H24V/H119F (*B*), and H36Q (*C*). All three curves are fitted with same pK_a values (Table 1), which are also used to fit the data in citrate buffer (Fig. 2), with reference values $k_u = 2 \times 10^{-5}$, $k_f = 6$ (*A*), $k_u = 2 \times 10^{-6}$, $k_f = 6$ (*B*), $k_u = 5 \times 10^{-4}$, and $k_f = 8$ (*C*). The rate constants are given in s^{-1}, and the reference values refer to pH 9.

fitted by the same pK_a values determined in citrate (Table 1), whereas the altered stability of I in acetate (Table 2) is taken into account by adjusting the values of k_u and k_f.

In analyzing the kinetics of a folding reaction, it is necessary to examine the kinetic amplitudes as well as the rates. The kinetic amplitudes in acetate buffer are shown in Fig. 4*A* for WT and in Fig. 4*B* for H24V/H119F. The unfolding or refolding reactions start at pH values where either N (unfolding) or I (refolding) is present in the initial conditions, and the pH-jump typically ends at pH values inside the unfolding transition zone, so that the final fluorescence value follows the equilibrium unfolding transition if the reaction is two-state. The fluorescence attributed to the two Trp residues in apoMb increases when N unfolds to I because of specific fluorescence quenching in N. The open and filled circles show the initial and final fluorescence values in refolding, whereas the open and filled squares show the initial and final values in unfolding. The final fluorescence values follow the equilibrium unfolding curve of N to I at pH values where only N and I are present, but, at lower pH values, U is also formed and the fluorescence again decreases. U has a lower fluorescence than I because the two Trp residues of apoMb are partially sequestered from solvent in I but are solvent exposed in U (16). The equilibrium pH unfolding curve obtained by monitoring fluorescence is subject to some uncertainty because of the difficulty of determining the correct unfolded and native base lines.

Table 1. pK_a values used to fit the pH-dependent unfolding/refolding kinetics

Residue	pK_a, N*	pK_a, I‡†	pK_a, I§	No.
His-24	>3.5	6.7	6.8	1
His-36	8.5	6.7	6.8	1
His-48	6.0	6.7	6.8	1
His-64	5.5	6.7	6.8	1
His-113	6.5	6.7	6.8	1
His-119	6.5	6.7	6.8	1
Acidic I	3.4	4.0	4.0	9
Acidic II	3.4	3.5	3.6	13

All pK_a values refer to 4.5°C, the temperature of the experiments reported here. The estimated uncertainty of the histidine pK_a values is ±0.1. See text for the procedure used to fix pK_a values of the acidic residues (Asp and Glu): group I corresponds to the unfolded CDEF subdomain of the apoMb molten globule, and group II corresponds to the structured A[B]GH subdomain of the molten globule.

*The pK_a values of histidine residues in native apoMb are taken from table 2 of ref. 2, determined at 35°C and corrected to 4.5°C (see text). No correction has been made for the possible influence of D_2O on the histidine pK_a values determined by chemical shift titration.

†The average pK_a value of histidine residues in the folding transition state, determined by fitting the plot of log k_{obs} versus pH for wild type in citrate buffer (Fig. 2A), when the pK_a values in N and in Ib are known.

§The average pK_a of the histidine residues in the molten globule, determined as shown in Fig. 1.

Quality of the Data Fitting. By using a single set of pK_a values to fit the pH-dependent unfolding/refolding kinetics not only of WT but also of the two mutants that unfold in different pH ranges (Fig. 3 *B* and *C*), we have a further test of the pK_a values. Likewise, using the same pK_a values to fit the kinetic data taken

Table 2. Properties of the pH-induced unfolding reactions in citrate vs. acetate buffer

	Citrate		Acetate	
Protein	pH_m	ΔG_{NI}	pH_m	ΔG_{NI}
WT	4.7	4.8	4.4	7.0
H24V/H119F	3.5*	7.2	3.2†	8.2
H36Q	n.d.	n.d.	5.3	5.3

Determined at 4.5°C in either 10 mM acetate or 2 mM citrate, 30 mM NaCl buffer. pH_m is the pH midpoint of the unfolding transition monitored by the final fluorescence values obtained in unfolding/refolding experiments, as in Fig. 4 *A* and *B*. ΔG_{NI} is the Gibbs energy difference between the native and molten globule forms at pH 9, in kcal/mol, computed from the values of k_u and k_f used to fit the curve of log k_{obs} vs. pH.

*A lower value than the one given here is obtained if the baseline found for the WT protein is used.

BIOPHYSICS

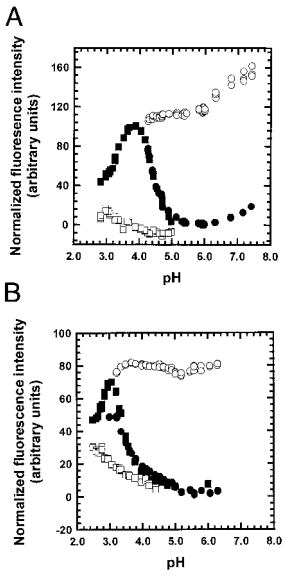

Fig. 4. The kinetic amplitudes of the unfolding and refolding experiments shown in Fig. 3 *A* and *B*. Open symbols are initial values, filled symbols are final values. Circles are refolding starting from pH 4.2, and squares are unfolding starting from pH 6.0. The fluorescence data are normalized so that the final fluorescence is 0 at pH 6.0 and 100 at pH 4.2. The fitted curves are equilibrium pH unfolding curves, which yield two of the pH_m values shown in Table 2

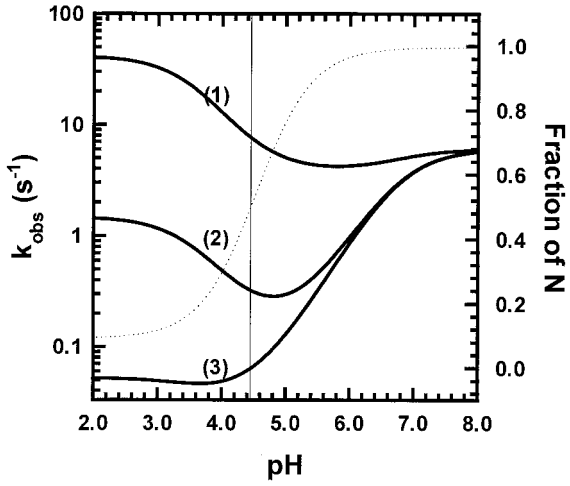

Fig. 5. Simulation of the values of k_{obs} vs. pH for a simple model (see text) in which only one ionizing group has pK_a values that differ in I, $I^{\ddagger}$, and N. The pK_a value in $I^{\ddagger}$ differs in the three cases shown: case 1, 6.6 (close to I); case 2, 5.15 (intermediate); case 3, 3.7 (close to N). The pK_a value in N is 3.5 and in I is 6.8 in all three cases. The fraction unfolded is shown on the right *y* axis, and the dotted line is the equilibrium unfolding curve (unfolding does not go to completion at low pH) calculated from the values of k_u and k_f vs. pH (see *Experimental Procedures*). Their values at pH 9 are $k_u = 0.001\ s^{-1}$ and $k_f = 6\ s^{-1}$.

in both acetate and citrate buffers provides an additional test of the pK_a values, because the location of the pH unfolding curve shifts significantly between acetate and citrate for both WT and H24V/H119F (Table 2). By insisting that a single set of pK_a values should fit all of the data, and by determining, one step at a time, the average pK_a values of the histidine residues in the Ib intermediate and in the folding transition state, we have a severe test of the assumptions made in this analysis as well as of the pK_a values. The fact that the fitted curve appears to be better for the double mutant (Figs. 2*B* and 3*B*) than for WT (Figs. 2*A* and 3*A*) probably reflects the fact that only one pK_a (the average pK_a of $I^{\ddagger}$) is an adjustable parameter in fitting the WT data, whereas the acidic pK_a values of both subdomains (Table 1) are adjusted in fitting the H24V/H119F data. The fitted curves for WT (Figs. 2*A* and 3*A*) diverge from the data points at low pH. The divergence can be eliminated by abolishing the carboxylate pK_a differences between different forms of the protein (I, $I^{\ddagger}$, and N), but then it becomes impossible to fit the pH-dependent unfolding refolding kinetics of H24V/H119F. The divergence occurs at pH values where unfolding ceases to be a two-state process, as the acid-unfolded form U becomes populated (compare Figs. 3*A* and 4*A*), and we tentatively assign the divergence to failure of the two-state assumption in this pH range. A second assumption that likely affects the quality of the fitted data is that the pK_a values are independent of the extent of titration of neighboring groups.

Simulation of the Effect of His-24 on the Unfolding/Refolding Kinetics. The fact that His-24 cannot be protonated in N gives this residue a unique role in the unfolding/refolding kinetics of WT, as shown by simulations for a simple model with only one ionizing residue. The pK_a of this residue in N is so low that its protonation cannot be observed. The rate curves in Fig. 5 are simulated for three different pK_a values in $I^{\ddagger}$: either 6.6 (curve 1), 5.15 (curve 2), or 3.7 (curve 3). The pK_a of the single residue is set at 3.5 in N and at 6.8 in I. The assigned pK_a of 3.5 in N does not allow this residue to be observably protonated in N because I is formed before N is protonated. The equilibrium transition curve for pH unfolding (dotted line in Fig. 5) is given by the ratio k_f/k_u, containing the rate constants for folding and unfolding, and pH_m, the pH midpoint of the equilibrium unfolding curve, is near 4.4, close to the experimental pH_m for WT in acetate. The unfolding transition does not go to completion at low pH because the assigned pK_a difference between N and I is not large enough to accomplish this when only a single residue is involved. The part of each simulated rate curve (Fig. 5) that lies below pH_m contributes to the unfolding rate whereas the part that lies above pH_m contributes to the refolding rate. The simulated curves show that the presence of a single residue whose pK_a differs substantially between N and I will have a large effect on the pH dependence of the unfolding/refolding kinetics.

The main qualitative features of the simulated results can be understood by noting two properties of the folding rate equation. First, at pH values below pH_m, the unfolding rate typically dominates the overall rate (the sum of the unfolding and refolding rates), whereas above pH_m the reverse is true. Second, the pK_a difference between N and $I^{\ddagger}$ controls the unfolding rate whereas the refolding rate is controlled by the pK_a difference between I and $I^{\ddagger}$. Thus, the refolding rate is nearly pH independent in case 1 (pK_a of $I^{\ddagger}$ is close to I), whereas the unfolding rate is nearly pH independent in case 3 (pK_a of $I^{\ddagger}$ is close to N). In case 2, (pK_a of $I^{\ddagger}$ intermediate between N and I) both the unfolding and refolding rates are strongly pH dependent. In experiments on pH-induced unfolding, the minimum value of the observed rate normally falls near the midpoint of the transition curve, as in denaturant-induced unfolding. The rate curve becomes independent of pH when the difference in number of protons bound becomes pH independent: for N versus $I^{\ddagger}$ if unfolding is being measured, and for I versus $I^{\ddagger}$ if refolding is being measured.

Discussion

Histidine pK_a Values Are Close to Model Compound Values in both I and $I^{\ddagger}$. The average pK_a of the histidine residues in the transition state (6.7) is close to the average pK_a in the molten globule (6.8; Table 1), and both pK_a values are determined by procedures in which only a single adjustable parameter is determined. The average histidine pK_a value determined for the molten globule is reasonably close to values measured in small peptides [6.8–6.9 at 25°C (17) or 7.2–7.3

at 4.5°C], considering that histidine pK_a values are affected significantly by neighboring charged residues (17, 18). In native apoMb, the range of pK_a values covers 3 pH units even when His-24 is excluded (see Table 1). Presumably the histidine residues in the molten globule are well exposed to solvent and do not make strong interactions with neighboring side chains, unlike histidine residues in the native protein. The effect of net charge on the pK_a values of the molten globule intermediate should be small at the pK_a of the histidine residues in I because the net proton charge is small: there are 15 basic groups, including histidines, and 13 acidic groups in the A[B]GH subdomain of apoMb. On the other hand, the pK_a values of His residues in holomyoglobin are affected by neighboring charged residues (17, 18), and they increase measurably with NaCl concentration (18).

Nature of the pH-Dependent Unfolding Kinetics of H24V/H119F. The double mutant H24V/H119F lacks His-24, and so its curve of log k_{obs} vs. pH might be expected to have a different shape from that of WT. Surprisingly, the two curves are similar in shape (Figs. 2 and 3). The Asp residues of native apoMb were studied by chemical shift titration of ^{13}C-labeled protein; 5 of 7 Asp residues could be observed and were found to titrate with normal pK_a values (2). No data for the Glu residues are available. The double mutant kinetic data can be fitted by assigning average pK_a values to the 9 Glu and Asp residues in the unfolded CDEF subdomain that are 0.6 pH units lower in N than in $I^{\ddagger}$ (Table 1). The effect on the pH-dependent unfolding rate is similar to that produced by the large (>3 pH) displacement of the pK_a of a single residue, His-24, in WT. The smaller increase in the refolding rate of H24V/H119F above pH_m can be fitted by assigning an average pK_a in $I^{\ddagger}$ to the 13 acidic groups in the A[B]GH subdomain that is only 0.1 pH units less than the average value in I.

The pK_a values assigned to the Asp and Glu residues (Table 1) are chosen on the basis of an earlier study of the acid-induced unfolding of the apoMb molten globule (19) that found that the Linderstrøm-Lang smeared-charge model describes reasonably well the effect of net positive charge on the stability of the molten globule, with w (the sole adjustable parameter of the model) = 0.05 and with an average value of 4.0 assigned to the intrinsic pK_a values of Asp and Glu. In that study, a set of single mutants, each with one basic residue mutated to alanine, consistently increased the stability of the molten globule if the positively charged group was inside the A[B]GH subdomain. Some additional mutants were studied later, and consistent results were found (20). The pK_a value of 3.6 assigned to 13 acidic residues (6 Asp, 7 Glu) in the A[B]GH subdomain is the value found from the Linderstrøm-Lang equation with $w = 0.05$. It agrees with the value ($pK_a = 3.54$) found by fitting data for the $I \rightleftharpoons U$ unfolding transition in figure 2 of ref. 21, by using equation 6 of ref. 2. The CDEF subdomain is treated as being unfolded, and its 9 acidic residues (1 Asp, 7 Glu and 1 C-terminal carboxylate included as being unfolded) are assigned a $pK_a = 4.0$. Then the values assigned to the average pK_a values in $I^{\ddagger}$ and N are obtained by fitting the experimental results.

The shift in pH_m between acetate and citrate (Table 2) is observed both with WT, whose unfolding occurs in a pH range where His-residues are titrating, and with H24V/H119F, whose unfolding occurs in a pH range where Asp and Glu residues are titrating. The similar behavior found in these two pH ranges indicates that the effect of anion binding is not restricted to one class of ionizing groups, and is consistent with the effect being one of net charge on molten globule stability. Preferential binding of the citrate anion, which would stabilize the molten globule by reducing its net positive charge (22), may account for the smaller value of ΔG_{NI} found in citrate versus acetate. Goto and Nishikori (23) carried out partial acetylation of lysine amino groups in cytochrome *c* and separated the partially reacted species by net charge using isoelectric focusing; they found that molten globule stability at pH 1.8 varies with net positive charge as expected if anion binding stabilizes molten globules.

Comparison with Related Work. The effect of protonating one residue (Asp 93) on the pH dependence of the unfolding rate of barnase was studied by Oliveberg and Fersht (10). They found a large rise in unfolding rate below pH_m and also a comparably large rise in refolding rate above pH_m, implying that the pK_a of Asp 93 in $I^{\ddagger}$ is roughly half way between its values in the native and denatured states. Our results are quite different, probably because there are important structural differences between barnase and apoMb. Charged Asp-93 in barnase forms part of a buried salt link with Arg-69, and its pK_a is strongly shifted in N, down to 0.7 in 50 mM KCl. The fact that the pK_a of Asp-93 in the folding transition state is intermediate between its values in the native and denatured states indicates that the ion pair interaction is formed but not fully developed in the transition state. In contrast to charged Asp 93 in barnase, neutral His-24 in apoMb forms a hydrogen-bonded interaction with His-119.

Concluding Comment. Residues with depressed pK_a values in the acid range are found commonly in studies of the pH dependence of stability of native proteins (24). They are thought to be a main contributor to the behavior, commonly observed in globular proteins, in which thermal stability drops sharply at acid pH (25). Our results suggest that the type of pH dependence found here for the $N \rightleftharpoons Ib$ reaction of apoMb, with a sharp rise in unfolding rate below pH_m and a smaller rise in refolding rate above pH_m, is likely to be found commonly in the kinetics of pH-dependent unfolding reactions of small proteins at acid pH, although the barnase results of Oliveberg and Fersht (10) show that this situation will not always occur.

This work was supported in part by research grants from the National Institutes of Health (GM 19988 to R.L.B.) and from the Deutsche Forschungsgemeinschaft (Ge 868/1-1 to B.H.G.).

1. Bashford, D., Case, D. A., Dalvit, C., Tennant, L. & Wright, P. E. (1993) *Biochemistry* **32**, 8045–8056.
2. Geierstanger, B., Jamin, M., Volkman, B. F. & Baldwin, R. L. (1998) *Biochemistry* **37,** 4254–4265.
3. Hennig, M. & Geierstanger, B. (1999) *J. Am. Chem. Soc.* **121,** 5123–5126.
4. Barrick, D., Hughson, F. M. & Baldwin, R. L. (1994) *J. Mol. Biol.* **237,** 588–601.
5. Takano, T. (1977) *J. Mol. Biol.* **110,** 537–568.
6. Hughson, F. M., Wright, P. E. & Baldwin, R. L. (1990) *Science* **249,** 1544–1548.
7. Cocco, M. J. & Lecomte, J. T. (1994) *Protein Sci.* **3,** 267–281.
8. Barrick, D. & Baldwin, R. L. (1993) *Biochemistry* **32,** 3790–3796.
9. Tanford, C. (1970) *Adv. Protein Chem.* **24,** 1–95.
10. Oliveberg, M. & Fersht, A. R. (1996) *Biochemistry* **35,** 6795–6805.
11. Loh, S. N., Kay, M. S. & Baldwin, R. L. (1995) *Proc. Natl. Acad. Sci. USA* **92,** 5446–5450.
12. Rossi-Fanelli, A., Antonini, E. & Caputo, A. (1958) *Biochim. Biophys. Acta* **30,** 608–615.
13. Edelhoch, H. (1967) *Biochemistry* **6,** 1948–1954.
14. Edsall, J. T. & Wyman, J. (1958) *Biophysical Chemistry* (Academic, New York).
15. Eaton, W. A., Muñoz, V., Hagen, S. J., Jas, G. S., Henry, E. R. & Hofrichter, J. (2000) *Annu. Rev. Biophys. Biomol. Struct.* **29,** 327–359.
16. Jamin, M. & Baldwin, R. L. (1998) *J. Mol. Biol.* **276,** 491–504.
17. Takahashi, T., Nakamura, H. & Wada, A. (1992) *Biopolymers* **32,** 897–909.
18. Kao, Y.-H., Fitch, C. A., Bhattacharya, S., Sarkisian, C. J., Lecomte, J. T. & Garcia-Moreno, B. (2000) *Biophys. J.* **79,** 1637–1654.
19. Kay, M. S. & Baldwin, R. L. (1998) *Biochemistry* **37,** 7859–7868.
20. Ramos, C. H. I., Kay, M. S. & Baldwin, R. L. (1999) *Biochemistry* **38,** 9783–9790.
21. Jamin, M., Antalik, M., Loh, S. N., Bolen, D. W. & Baldwin, R. L. (2000) *Protein Sci.* **9,** 1340–1346.
22. Goto, Y., Takahashi, N. & Fink, A. L. (1990) *Biochemistry* **29,** 3480–3488.
23. Goto, Y. & Nishikori, S. (1991) *J. Mol. Biol.* **222,** 679–686.
24. Anderson, D. E., Lu, J., McIntosh, L. & Dahlquist, F. W. (1993) in *NMR of Proteins: Topics in Molecular and Structural Biology*, eds. Clore, G. M. & Gronenborn, A. M. (CRC, Boca Raton), pp. 258–304.
25. Privalov, P. L. (1979) *Adv. Protein Chem.* **33,** 167–241.